Articles

Discovery of (2*R*)-2-(3-{3-[(4-Methoxyphenyl)carbonyl]-2-methyl-6-(trifluoromethoxy)-1*H*-indol-1-yl}phenoxy)butanoic Acid (MK-0533): A Novel Selective Peroxisome Proliferator-Activated Receptor γ Modulator for the Treatment of Type 2 Diabetes Mellitus with a Reduced Potential to Increase Plasma and Extracellular Fluid Volume

John J. Acton, III, Taro E. Akiyama, Ching H. Chang, Lawrence Colwell, Sheryl Debenham, Thomas Doebber, Monica Einstein, Kun Liu, Margaret E. McCann, David E. Moller,† Eric S. Muise, Yugen Tan, John R. Thompson, Kenny K. Wong, Margaret Wu, Libo Xu, Peter T. Meinke, Joel P. Berger, and Harold B. Wood*

Merck Research Laboratories, Merck & Co., Inc., RY800-C114, P.O. Box 2000, Rahway, New Jersey 07065

Received January 23, 2009

Peroxisome proliferator-activated receptor gamma (PPARγ) agonists are used to treat type 2 diabetes mellitus (T2DM). Widespread use of PPARγ agonists has been prevented due to adverse effects including weight gain, edema, and increased risk of congestive heart failure. Selective PPARγ modulators (SPPARγMs) have been identified that have antidiabetic efficacy and reduced toxicity in preclinical species. In comparison with PPARγ full agonists, SPPARγM **6** (MK0533) displayed diminished maximal activity (partial agonism) in cell-based transcription activation assays and attenuated gene signatures in adipose tissue. Compound **6** exhibited comparable efficacy to rosiglitazone and pioglitazone in vivo. However, with regard to the induction of untoward events, **6** displayed no cardiac hypertrophy, attenuated increases in brown adipose tissue, minimal increases in plasma volume, and no increases in extracellular fluid volume in vivo. Further investigation of **6** is warranted to determine if the improvement in mechanism-based side effects observed in preclinical species will be recapitulated in humans.

Introduction

Type 2 diabetes mellitus (T2DM[a]) is a metabolic disorder characterized by insulin resistance and hyperglycemia. Historically, the disease has been associated with obesity resulting from the sedentary western lifestyle. However, the incidence of T2DM is quickly emerging as a global medical concern. If the incidence of T2DM continues unchecked at its current rate, the World Health Organization predicts there will be 300 million cases worldwide by the year 2010. While lifestyle changes would significantly ameliorate the risk or severity of this disease state, compliance with existing therapies remains a long-standing problem owing to generally poor tolerability of most T2DM targeted drugs. One class of effective chemotherapeutic agents for T2DM is the thiazolidinediones (TZDs, e.g., rosiglitazone and pioglitazone). These compounds function as sensitizers of endogenous insulin via activation of the peroxisome proliferator activated receptor gamma (PPARγ). PPARγ is a member of the nuclear hormone receptor super family. There are two PPARγ subtypes (PPARγ1/PPARg2). PPARγ1 is expressed at low levels in many tissues, while PPARγ2 is highly expressed in adipocytes. The full potential of these drugs has not been realized due to undesirable weight gain, peripheral edema, and anemia (resulting from increased plasma volume) following prolonged usage.[1,2] These adverse effects have precluded dosing TZDs to achieve maximal clinical efficacy and ruled out their wider usages. Indeed, TZDs are contra-indicated for T2DM patients who are at risk for congestive heart failure because the fluid retention they induce can exacerbate this disease.[3] Similar side effects have been observed in rodents as well,[4] and more recently additional concerns have been raised over generally increased cardiovascular risk[5,6] and possible loss of bone mass following TZD treatment.[7,8]

Considering the beneficial insulin sensitizing effects of TZD therapy, a significant effort has been devoted to the development of selective PPARγ modulators (SPPARγMs) that retain the desirable efficacy for type 2 diabetes but have diminished potential for, or ideally lack all together, the undesirable PPARγ mechanism-based side effects.[3,9−18] Herein, we describe our efforts to identify an optimized indole-derived SPPARγM (**6**, MK-0533) that demonstrates a reduced potential to cause increases in heart weight, plasma volume, and extracellular fluid volume and is equally efficacious to rosiglitazone and pioglitazone in its ability to improve diabetes in animal models. SPPARγM **6** has an ancillary profile suitable to allow its evaluation of in man.

In Vitro SAR and Synthesis. We recently have disclosed a preliminary summary describing a structurally novel series of SPPARγMs.[19,20] A thorough investigation of the SAR revealed that the key features exemplified in Figure 1 were critical for SPPARγM activity. These SPPARγMs are potent partial agonists in cell-based transcriptional activity assays that, in

* To whom correspondence should be addressed. Phone: 732 594 7592. Fax: 732 594 9556. E-mail: blair_wood@merck.com.
† Current address: Lilly Research Laboratories, Lilly Corporate Center, DC 0545, Indianapolis, Indiana 46285.

[a] Abbreviations: PPARγ, peroxisome proliferator-activated receptor γ; T2DM, type 2 diabetes mellitus; SPPARγM, selective peroxisome proliferator-activated receptor γ modulator; TZD, thiazolidinedione; CYP, cytochrome P450; SPA, scintillation proximity assay; PV, plasma volume; ECF, extracellular fluid; TG, triglyceride; FFA, free fatty acid; HW, heart weight.

10.1021/jm900097m CCC: $40.75
Published on Web 06/09/2009

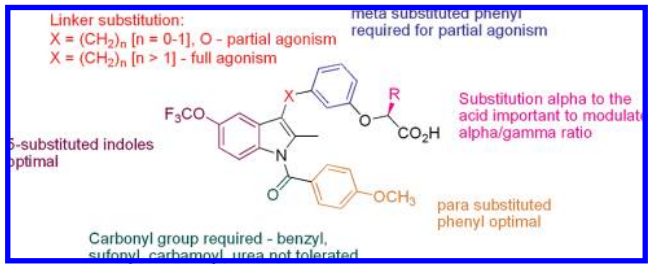

Figure 1. Summary of SAR of the indolyl SPPARγMs.

comparison with full agonists, produce a diminished gene signature in 3T3-L1 adipocytes and display a decreased ability to induce adipogenic differentiation of cultured rodent and human preadipocytes.[21] The observation that full and partial agonists interact differently with PPARγ suggests that ligand−receptor complexes with SPPARγMs may show quantitatively different interactions with coactivators and corepressors, thereby providing a physical basis for their differing pharmacological profiles. However, the ancillary profiles of the compounds disclosed to date were ill suited to merit clinical investigation of these compounds in type 2 diabetic subjects. Thus, refining the search for optimized SPPARγMs with more suitable drug-like ancillary profiles was a necessary prerequisite prior to considering evaluation of the potential benefits of these compounds in type 2 diabetic subjects.

With the structural elements for potent in vitro SPPARγM activity identified, we turned our attention to the optimization of the ancillary profile of these molecules. A major liability of the *N*-benzoyl indoles was significant loss of the labile anisoyl group after oral dosing in rats. This liability was exacerbated, as the resultant indole metabolites were potent CYP inhibitors and found to accumulate after multiple dosing, raising the risk for significant drug−drug interaction liabilities (Figure 2).

As the carbonyl oxygen of **1** was integral for binding potency, fused heterocycles were evaluated as possible isosteric replacements for the benzoyl group. Extensive modification of each series to maximize intrinsic activity and introduce additional desirable, drug-like properties was undertaken; the following compounds (**2**−**6**) exemplify optimal derivatives from a given cohort. For instance, a benzisoxazole proved to be a suitable replacement for the anisoyl moiety. Although the optimized *N*-benxisoxazole SPPARγM **2** was equipotent to the benzoyl indoles in vitro and in vivo, low levels of the parent indoles lacking *N*-substitution (similar to **1a**) were still detected systemically in plasma after orally dosing compounds such as **2**. Therefore, further scaffold refinements were investigated to avoid this troubling P-450 liability. 1,3-Transposition of the indole nucleus such that the benzoyl group was connected via a carbon−carbon bond at the 3-position of the indole provided analogue **3**, which is now incapable of debenzoylation in vivo. This reversed indole maintained potent partial agonist activity in vitro. However, **3** was found to have poor bioavailability, low systemic plasma exposure, high clearance, and a short half-life in preclinical species. In an effort to improve its pharmacokinetic profile, additional modification of the reversed indole platform was initiated. Hybrid analogues were synthesized in which the benzisoxazole functionality was incorporated onto the 3-position of the transposed indole core. Such analogues, typified by **4**, while demonstrating good in vitro potency with improved pharmacokinetic characteristics overall had comparatively modest efficacy in rodent models of diabetes. While in general terms, this modification was viable, hybrid analogue **4** subsequently was found to have undesirable off-target activities, primarily inhibition of simvastatin acid glucuronidation. The comparatively high systemic plasma exposures required for useful in vivo efficacy raised concerns for potential drug−drug interactions with simvastatin, therefore more scaffold optimization ensued.

The reversed indole platform offered greater opportunity to probe modifications to the carbonyl/benzisoxazoyl region. Introducing an aryl ether in place of the benzoyl or benzisoxazoyl group afforded potent partial agonists in vitro and in vivo. However, 3-phenoxy indole **5** was poorly tolerated in vivo with unacceptable increases in liver enzymes (e.g., ALT and AST) detected after 2 weeks dosing in a rat tolerability assay. Ultimately, a desirable ancillary profile was realized after revisiting the reversed indole scaffold containing a 3-benzoyl substituent. An improved pharmacokinetic profile could be obtained by excising the methylene moiety and directly attaching the phenyl ring to the nitrogen of the indole ring system to yield compound **6**. Compound **6** was a potent PPARγ selective partial agonist in vitro, was not a potent inhibitor of the P-450 enzymes (>10 uM against all CYPs), was not a time-dependent inhibitor of CYP3A4, and demonstrated low irreversible protein binding in vitro (<10 pmol/mg protein in rat and human liver microsomes) and in vivo in rat (<10 pmol/mg protein in plasma and liver).[22]

SPPARγM **6** was evaluated in vitro in PPAR assays from multiple species and was found to be a potent ligand for hPPARγ in SPA-based assays and a partial agonist of PPARγ in cell-based transcriptional assays with high selectivity for PPARγ over PPARα (Table 2). Using the human isoforms, >600 times more selectivity was observed between PPARγ versus PPARα. In preclinical species, **6** also demonstrated good selectivity between PPARγ and PPARα (>48 times) in vitro. All the compounds described here demonstrated a high degree of selectivity over PPARδ subtype. No activity was observed for this receptor at the highest concentration tested (10 μM) in the binding assay.

We have also evaluated SPPARγM **6** in gene expression studies performed in fully differentiated 3T3-L1 adipocytes using Agilent 25K spotted microarrays. At PPARγ saturating concentrations, SPPARγM **6** showed an overall similar but attenuated gene expression profile compared with the PPARγ full agonists rosiglitazone and non-TZD carboxylic acid PPARγ agonist (COOH).[23] No robust SPPARγM **6** specific signature genes were observed (Figure 3). A PPARγ activity score was developed using a χ-square fitting approach and a set of 4619 reporter genes in order to provide a single relative measure of the magnitude of their expression and therefore PPARγ activation.[23] These 4619 reporter genes represent the intersection of the two structurally distinct PPARγ full agonists rosiglitazone and COOH at $p < 0.01$, which we believe represents a "true" PPARγ target gene signature (both directly and indirectly regulated genes) in the adipocytes. While the activity scores of full agonists were indistinguishable (both rosiglitazone and COOH have scores of 1.0), the activity score of SPPARγM **6** was 0.62 (Table 2, last entry) due to the attenuated PPARγ gene expression profile relative to that of rosiglitazone.

SPPARγM **6** was prepared in good overall yields and high enantiopurity utilizing the route outlined in Scheme 1. The core indole was prepared via a Gassman indole synthesis[24] to provide **8** in 40−60% isolated yields, subsequent to removal of the undesired regioisomer. *N*-arylation of **8** with 3-bromoanisole was achieved using a catalytic Pd/ligand cocktail to afford **10** in high yields after demethylation with boron tribromide. Acylation at the 3-position with anisoyl chloride and diethyl

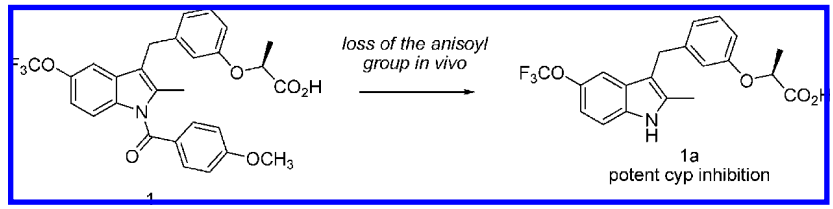

Figure 2. *N*-Acyl indoles are metabolically labile in vivo.

Table 1. Human PPARγ Binding IC_{50} and Transactivation EC_{50} Values

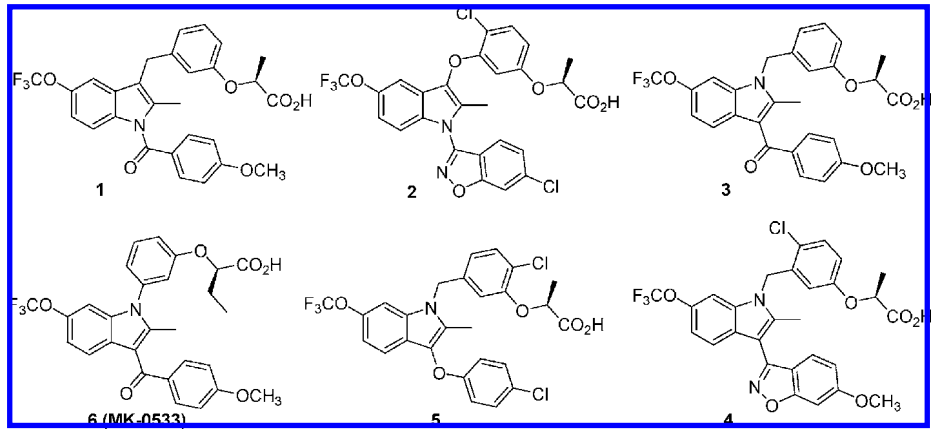

compd	IC_{50} (nM)[a]	EC_{50} (nM)[b]	% max activation	features
rosiglitazone	~200	20−27	100	full agonist
1	1	2	36	labile benzoyl
2	6	3	31	labile benzisoxazole
3	1	1	25	poor PK profile
4	2	3	24	off-target activity
5	1	3	20	poor rodent tolerabilty
6	9	2	25−39%	optimized scaffold

[a] IC_{50} is measured by the complete displacement of a radio-labeled full agonist indicating competitive binding to the receptor in a SPA assay format. [b] EC_{50} is defined as the compound concentration at which 50% of a given compound's intrinsic maximal response has been reached.

Table 2. Comparison of SPPARγM 6 and Rosiglitazone in Vitro Potencies across Species and PPARγ Activity Score Based upon Gene Expression in 3T3-L1 Adipocytes

in vitro potencies (nM)	SPPARgM **6**	rosiglitazone
hPPARγ (IC_{50})[a,b]	9−14	~200
hPPARα (IC_{50})[b]	>50000	>50000
hPPARγ (EC_{50})[c]	2−5 (42−68%)	20−27
hPPARα (EC_{50})[c]	33−68% @ 3000	1−4% @ 3000
murine PPARα (EC_{50})[c]	240−340 (53−64%)	na
hamster PPARα (EC_{50})[c]	330−440 (52−80%)	na
dog PPARα (EC_{50})[c]	370 (35−62%)	na
PPARγ activity score	0.6	1.0

[a] PPARγ binding is similar across all species evaluated. Only human binding data is presented for clarity. [b] IC_{50} is measured by the complete displacement of a radio-labeled full agonist indicating competitive binding to the receptor in a SPA assay format. [c] EC_{50} is defined as the compound concentration at which 50% of a given compound's intrinsic maximal response has been reached.

aluminum chloride followed by a basic workup of the reaction provided intermediate **11**. Coupling the phenol with *tert*-butyl (*S*)-2-hydroxy butyrate afforded the desired acid **6** in high yields and high enantiomeric excess after removal of the *tert*-butyl ester with trifluoroacetic acid (Scheme 1).[25]

Pharmacokinetics. Overall, **6** was found to have desirable pharmacokinetic characteristics in preclinical species with low to moderate plasma clearance, moderate to good oral bioavailability, and acceptable terminal half-life (Table 3).

Efficacy in *db*/*db* Mice. To evaluate its antidiabetic efficacy in vivo, SPPARγM **6** was dosed in *db*/*db* mice, an obese insulin resistant rodent model of T2DM characterized by hyperglycemia and hypertriglyceridemia.[26] Its in vivo efficacy was compared to rosiglitazone and pioglitazone as positive controls; the dosage of each agent was selected such that comparable efficacy was obtained in all treatment groups. After once daily oral dosing for 11 days, compound **6** produced a significant reduction in blood glucose levels (−83%). Rosiglitazone and pioglitazone performed similarly, affording glucose decrements of 75% and 50%, respectively. On the final day of dosing, the systemic plasma exposures of each compound were measured. It is noteworthy that despite the in vitro partial agonist activity in transactivation assays and attenuated gene signature in adipocytes relative to rosiglitazone, based upon the systemic plasma drug exposure, SPPARγM **6** was roughly 3−5 times more potent than pioglitazone or rosiglitazone in this diabetic animal model (Table 4). Plasma levels of adiponectin, a bona fide PPARγ target engagement biomarker, also were measured in the rosiglitzone and SPPARγM treatment groups. Significant increases in adiponectin were observed in both treatment groups.

Tolerability in Sprague−Dawley Rats. Recently, reports have emerged that rosiglitazone causes increased risk of cardiovascular complications after prolonged usage in humans.[5,6] Also, thiazolidinediones have been associated with cardiac hypertrophy in a number of preclinical species.[27] To evaluate if the partial agonist activity would translate into a different in vivo profile, SPPARγM **6** was compared head-to-head with rosiglitazone in Sprague−Dawley rats. Both agents were dosed daily for 2 weeks at dosages to achieve exposures that were

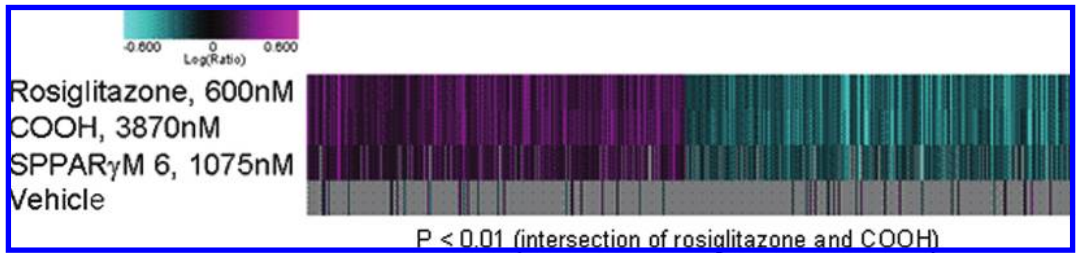

Figure 3. Comparison of rosiglitazone, COOH, and SPPARγM **6** gene expression heat map of 4619 reporter genes.

Scheme 1. Synthesis of SPPARγM **6**

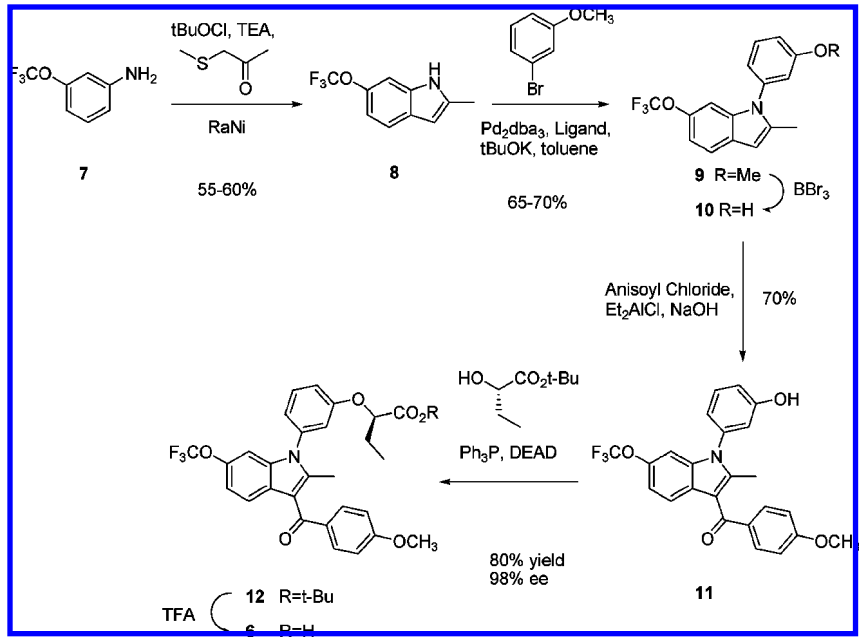

Table 3. Pharmacokinetic Profile of SPPARγM **6** in Preclinical Species

species	% *F*	PO nAUC (μM·h)	Clp (mL/min/kg)	$T_{1/2}$ (h)	C_{max} (μM)	Vdss (L/kg)
rat	81	1.6	18.3	1.6	1.0	1.4
dog	59	2.9	7.5	3.6	2.4	1.4
monkey	25	0.8	10.1	3.2	0.5	0.7

about 10 times greater than the dosages administered to *db*/*db* mice in efficacy studies. In contrast to rosiglitazone, which produced the expected increases in heart weight (25%) and brown adipose tissue (BAT, 260%), there was no significant increase in heart weight observed in animals dosed with SPPARγM **6**. Another distinguishing characteristic was the diminished augmentation in BAT weight by **6** in comparison to rosiglitazone. Overall, SPPARγM **6** was well tolerated and there were no significant findings other than a nominal increase in liver weight (120%) comparable to that observed with the PPARα agonist fenofibrate, which was also included as a control. The increases in liver weight after treatment with **6** reflect the minor murine PPARα activity present with this compound (Table 4).

Evaluation of Plasma Volume and Extracellular Fluid Volume Increases in *fa*/*fa* Zucker Rats. On the basis of its robust efficacy in *db*/*db* mice and the unique tolerability profile in Sprague−Dawley rats, further in vivo characterization of SPPARγM **6** was undertaken. To evaluate its potential for mechanism-based side effects, we examined two parameters in obese *fa*/*fa* Zucker rats, plasma volume (PV) and extracellular fluid volume (ECF) augmentation, that have previously been used as surrogate markers for induction of edema by PPARγ agonists.[23] Briefly, changes in plasma volume are determined by Evan's blue dye dilution, while ECF volume changes are determined by bioelectrical impedance. Although not frankly diabetic, insulin resistant *fa*/*fa* Zucker rats are hyperinsulinemic and dyslipidemic. Therefore, the use of this model makes it possible to evaluate both the insulin sensitizing and mechanism-based side effects of PPARγ ligands in the same model.

Table 4. Evaluation of SPPARγM **6** in *db*/*db* Mice and Sprague−Dawley Rats[a]

	db/*db* mouse			
compd	vehicle	rosiglitazone	**6**	pioglitazone
dose (mpk)		10	30	75
AUC (μM·h)		320	60	205
gluc. correction (%)		−79 ± 10	−83 ± 4	−50 ± 11
adiponectin (μg/mL)	14.5 ± 1.7	57.3 ± 3.1[b]	48.1 ± 6.8[b]	n.d.[d]

	Sprague−Dawley rat			
compound	vehicle	rosiglitazone	**6**	fenofibrate
dose (mpk)		150	300	300
AUC (μM·h)		581	954	5582
heart (g)	1.12 ± 0.03	1.39 ± 0.07[b]	1.10 ± 0.03	1.16 ± 0.04
liver (g)	9.0 ± 0.4	10.5 ± 0.8	19.7 ± 0.9[b]	18.9 ± 0.3[b]
BAT[c] (mg)	263 ± 13	944 ± 145[b]	537 ± 35[b]	276 ± 41

[a] Values are the means of six animals/group ± the standard error of the mean. [b] $P < 0.05$ compared to vehicle controls (Dunnett's *t* test). [c] BAT = brown adipose tissue. [d] nd = not determined.

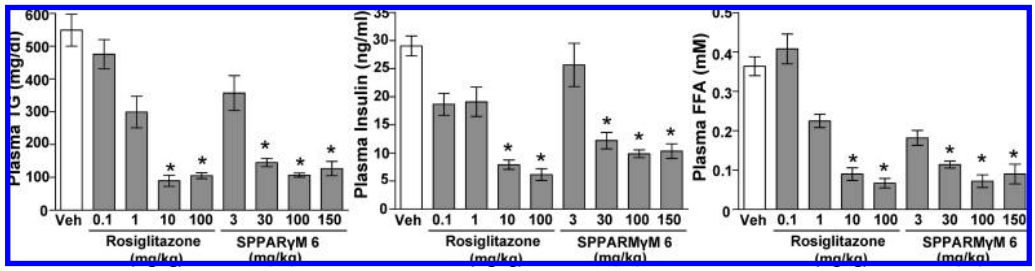

Figure 4. Comparison of TG, insulin, and FFA lowering between rosiglitazone and SPPARγM **6** in Zucker *fa*/*fa* rats. * $P < 0.05$ compared to vehicle controls (Dunnett's *t* test).

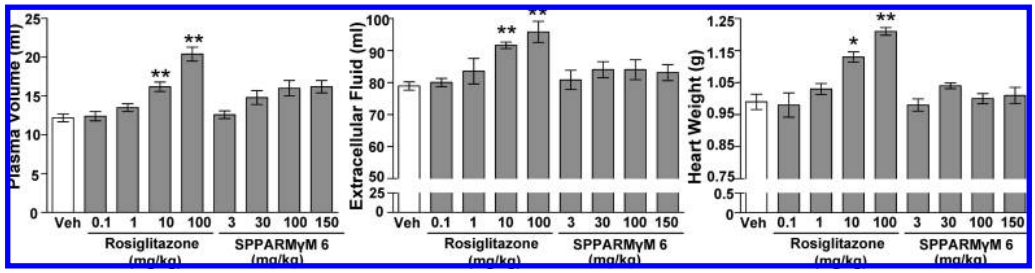

Figure 5. Comparison of PV, ECF, and HW increases between rosiglitazone and SPPARγM **6** in Zucker *fa*/*fa* rats. * $P < 0.05$, ** $P < 0.01$ compared to vehicle controls (Dunnett's *t* test).

Following 7 days of treatment with either rosiglitazone or **6** in Zucker *fa*/*fa* rats, the final body weights of treatment groups were not statistically different from those of *fa*/*fa* vehicle controls. In general, body-weight gain correlated well with food consumption over the study period regardless of treatment group. Plasma glucose levels were not elevated in the vehicle control *fa*/*fa* Zucker rats and were unaffected by rosiglitazone or SPPARγM **6**. Plasma trigylcerides (TG), insulin, and free fatty acids (FFA) were significantly reduced by rosiglitazone, and SPPARγM **6** indicative of diminished insulin resistance. As shown in the graphs, rosiglitizone affords maximal reductions in plasma TG, insulin, and FFA at 10 mpk with no further decreases upon increasing the dosage to 100 mpk. Similar reductions in TG, insulin, and FFA are observed at the 30 mpk dosage of SPPARγM **6**. At the end of the study period, systemic plasma drug levels were measured at each dosage. The exposures for rosiglitazone were 9.0, 61.1, 583.7, and 6458 μM·h at 0.1, 1, 10, and 100 mg/kg, respectively. The plasma exposures for SPPARγM 6 were 6, 115.2, 1475, and 4522 μM·h at 3, 30, 100, and 150 mg/kg, respectively. Compound dose ranges were selected based upon differences in mouse and rat PK as well as the dosage needed for efficacy in *db*/*db* mouse. On an exposure basis, SPPARγM **6** is 5 times more potent that rosiglitazone when dosed to achieve maximal reductions in TG, insulin, and FFA. This is consistent with the findings in *db*/*db* mice (Figure 4).

Significant increases in PV, ECF volume, and heart weight (HW) were observed at the 10 mpk dosage of rosiglitazone, and further increases in these parameters occur at the 100 mpk dosage. After treatment with SPPARγM **6**, no significant increase in PV was observed at the 30 mpk dosage. However, there was a modest increase in PV with SPPARγM **6** at 100 mpk, but in contrast to rosiglitazone, this augmentation reached a plateau upon increasing the dosage up to 150 mpk. Furthermore, SPPARγM **6** did not produce any significant increases in ECF or HW at any dosage evaluated. On the basis of these findings, we conclude that SPPARγM **6** afforded efficacy comparable to rosiglitazone with reduced potential for mechanism-based side effects (Figure 5).

Summary

Herein we describe the identification of a novel indole-derived SPPARγM. In contrast to full agonists, SPPARγM **6** was a partial agonist in cell-based transcriptional activity assays and produced an attenuated gene signature in 3T3-L1 adipocytes. In a widely accepted rodent model of diabetes, *db*/*db* mice, SPPARγM **6** exhibited comparable efficacy to rosiglitazone and pioglitazone. It also showed similar insulin sensitizing activity to PPARγ full agonists in insulin resistant *fa*/*fa* Zucker rats. However, with regard to the induction of adverse events, SPPARγM **6** displayed a number of important benefits vs rosiglitazone. No cardiac hypertrophy was seen, and only attenuated increases in brown adipose tissue were noted after treating Sprague−Dawley rats chronically with high dosages of **6**. In Zucker *fa*/*fa* rats, SPPARγM **6** treatment produced only a trend toward increased plasma volume that plateaued with increasing doses, while concomitant increases in extracellular fluid or heart weight were not observed. The robust preclinical antidiabetic activity and superior ancillary pharmacology of SPPARγM **6** is sufficient to merit further investigation of its properties and to determine if the improvement in mechanism-based side effects observed in preclinical species will be recapitulated in humans.

Experimental Section

General. All commercial chemicals and solvents were reagent grade and were used without further purification unless otherwise specified. All reported yields were isolated yields after chromatography or crystallization. NMR spectra were obtained on a Varian Inova 500 MHz NMR spectrometer equipped with either a Nalorac 3 mm probe or a Varian indirect detection 3 mm probe. All spectra run in $CDCl_3$ were referenced to residual $CHCl_3$ at δ 7.26 ppm. Standard resolution mass spectra were obtained on HP1100 LC/MS systems; all mass spectra were obtained using electrospray ionization (EI) in positive ion mode. An LCT time-of-flight mass spectrometer (Waters, Beverly MA) with LockSpray electrospray ionization source was used for exact mass analysis. Chemical purity and enantiopurity was confirmed by HLPC to be >95%. Purity was determined by HPLC analysis via gradient elution (10%−100% acetonitrile/water modified with 0.1% TFA over 3 min with a 30 s

hold at 100% acetonitrile followed by a return to 10% acetonitrile/water in 30 s at 5 mL/min) on a YMC C8 column (5 μm) at λ = 220 nm. Chiral purity determined by treating (**6**) with TMS-diazomethane and isolating the methyl ester. Chiral HPLC analysis of the methyl ester was performed using 85% heptane/15% EtOH as eluent on a Chiralpak AD column (4.6 mm × 250 mm) at a flow rate of 0.75 mL/min using a photodiode array detector, plus single wavelength analysis at 254 nm. The methyl ester of racemic (**6**) was also prepared for comparison.

2-Methyl-6-(trifluoromethoxy)-1*H*-indole (8) step 1. To a vigorously stirred solution of 3-trifluoromethoxyaniline (**7**, 5.74 g, 0.032 mol) in methylene chloride (100 mL) at −78 °C (acetone−dry ice bath) was added dropwise a solution of *tert*-butyl hypochlorite (3.5 g, 0.032 mol) in 15 mL of the same solvent. After 10 min, a solution of methylthio-2-propanone (3.375 g, 0.032 mol) in methylene chloride (15 mL) was added slowly over 10 min. A slight exotherm was noted during the addition, resulting in a clear yellow solution. After stirring for another hour at −78 °C, during which time the intermediate azasulfonium salt precipitated to form a suspension, a solution of triethylamine (4.5 mL, 0.032 mol) in methylene chloride (15 mL) was added slowly over 5 min to give a clear solution. After an additional 10 min at −78 °C, the cooling bath was removed and the reaction was allowed to warm to room temperature. A 50 mL portion of water was added under vigorous stirring, and the organic layer was separated, dried over anhydrous $MgSO_4$, filtered, and concentrated in vacuo to give 8.75 g of a 2:1 mixture of the desired 6-triluoromethoxy-2-methyl-3-methylthio-indole and the corresponding 4-trifluoromethoxy isomer as a yellow oil. The crude product was used in the next step without further purification. LC-MS (M + 1) 262.

2-Methyl-6-(trifluoromethoxy)-1*H*-indole (8) Step 2. A solution of the crude product from the previous step (8.8 g, 0.032 mol) in 250 mL of absolute ethanol was placed in a 500 mL, three-necked, round-bottomed flask fitted with a mechanical stirrer. An excess of freshly washed W-2 Raney nickel (80 g, 50% slurry in water, washed twice with water and three times with ethanol) was added. The mixture was stirred for 4 h (the reaction was monitored by LC-MS). The Raney nickel was removed by filtration through celite and washing with ethanol. (CAUTION: W-2 Raney nickel may ignite spontaneously if allowed to become dry. During the filtration, a small amount of solvent must be left to cover the catalyst.) The combined ethanolic solutions were concentrated in vacuo. Purification by flash chromatography (Biotage 75 Flash, 9:1 hex/EtOAc) gave 4.05 g of the desired product as white solid (58.1%) and 2.0 g of the 4-trifluoromethoxy indole isomer as an oil (28.7%). ^{1}H NMR ($CDCl_3$, 500 MHz): δ 7.93 (br s, 1H), 7.45 (d, J = 8.6 Hz, 1H), 7.16 (s, 1H), 6.95 (d, J = 8.6 Hz, 1H), 6.23 (s, 1H), 2.45 (s, 3H). LC/MS: *m*/*e* 215.89 (M + 1). HRMS: *m*/*e* 216.0628 (M + 1) calcd (M + 1) 216.0636.

1-(3-Methoxyphenyl)-2-methyl-6-(trifluoromethoxy)-1*H*-indole (9). 2-Methyl-6-(trifluoromethoxy)-1*H*-indole (**8**), 645 mg, 3.0 mmol), 3-bromoanisole (0.456 mL, 3.6 mmol), sodium *t*-butoxide (404 mg, 4.2 mmol), trisdibenzylidine dipalladium (206 mg, 0.225 mmol), and 2-di-*t*-butylphosphinobiphenyl (201 mg, 0.675 mmol) were stirred in toluene at 80 °C and monitored by TLC (3/1 hexanes/methylene chloride) or reversed phase HPLC until complete. The reaction mixture was then cooled, filtered over celite, and the filtrate evaporated to give a crude isolate, which was purified by silica gel chromatography to give the title compound (460 mg, 48% yield). ^{1}H NMR (500 MHz, $CDCl_3$): δ 7.51 (d, Ph, J = 8.5 Hz, 1H), 7.45 (t, Ph, 1H), 7.02 (dd, Ph, J = 8.4, 2.5 Hz, 1H), 6.99 (m, Ph, 2H), 6.92 (dd, Ph, J = 8.3, 1.6 Hz, 1H), 6.86 (t, Ph, 1H), 6.39 (s, Ph, 1H), 3.85 (s, OCH_3, 3H), 2.30 (s, 2-CH_3, 3H). LC/MS: *m*/*e* 322.05 (M + 1).

3-[2-Methyl-6-(trifluoromethoxy)-1*H*-indol-1-yl]phenol (10). First, 460 mg (1.43 mmol) of (**9**) was dissolved in 7 mL of dichloromethane at 0 °C. Then boron tribromide (1.0 N, 2.86 mL) in dichloromethane was added, the cooling bath was removed, and the reaction was stirred at room temperature overnight. The reaction was then quenched with ice for 30 min and partitioned. The organic was washed with water and dried over sodium sulfate. After filtering the drying agent, the filtrate was evaporated and the residue purified by silica gel chromatography to give 397 mg (90%) of the title compound. ^{1}H NMR (500 MHz, $CDCl_3$): δ 7.50 (d, Ph, J = 8.5 Hz, 1H), 7.41 (t, Ph, 1H), 6.99 (d, Ph, J = 8.5 Hz, 1H), 6.97 (s, Ph, 1H), 6.94 (dd, ph, J = 8.2, 2.5 Hz, 1H), 6.91 (dd, Ph, J = 7.5, 1.4 Hz, 1H), 6.81 (t, Ph, 1H), 6.38 (s, Ph, 1H), 5.02 (s, OH, 1H), 2.30 (s, 2-CH_3, 3H).

[1-(3-Hydroxyphenyl)-2-methyl-6-(trifluoromethoxy)-1*H*-indol-3-yl](4-methoxyphenyl)methanone (11). First, 242 mg (0.788 mmol) of (**10**) was dissolved in methylene chloride (4 mL) and cooled to −20 °C. Then a solution of diethylaluminum chloride in toluene (1.8M, 1.23 mL) was added slowly (over 1−2 min) and stirred for 5−15 min. Then added a solution of 4-methoxybenzoyl chloride (377 mg, 2.21 mmol) in methylene chloride (1 mL) and allowed to stir overnight while slowly reaching room temperature. pH 7.0 buffer was added dropwise until gas evolution ceased and then partitioned. The aqueous layer was extracted twice more with methylene chloride, and then the combined organic layers were washed twice with saturated NaCl solution, dried over sodium sulfate, filtered, and evaporated. The crude isolate was then dissolved in methanol (5 mL), and sodium hydroxide solution (1.0 M, 1.6 mL) was added. The solution was monitored by TLC for disappearance of diacyl indole and then neutralized with HCl (1.0 M, 1.6 mL). The reaction mixture was then diluted with water and extracted with ethyl acetate. The ethyl acetate layer was dried over sodium sulfate, filtered, evaporated, and the residue purified by silica gel chromatography to give 222 mg (64% yield) of the title compound. ^{1}H NMR (500 MHz, $CDCl_3$): δ 7.83 (d, Ph, J = 8.8 Hz, 2H), 7.45 (t, Ph, 1H), 7.41 (d, Ph, J = 8.6 Hz, 1H), 7.05 (dd, Ph, J = 8.8, 2.4 Hz, 1H), 6.97 (m, Ph, 3H), 6.94 (s, Ph, 1H), 6.91 (dd, Ph, J = 8.5, 1.4 Hz, 1H), 6.86 (t, Ph, 1H), 6.38 (s, OH, 1H), 3.91 (s, OCH3, 3H), 2.35 (s, 2-CH_3, 3H). HRMS: *m*/*e* 442.1267 (M + 1) calcd (M + 1) 442.1266.

***tert*-Butyl(2*R*)-2-(3-{3-[(4-methoxyphenyl)carbonyl]-2-methyl-6-(trifluoromethoxy)-1*H*-indol-1-yl}phenoxy)butanoate (12).** First, 220 mg (0.500 mmol) of (**11**) was dissolved in tetrahydrofuran (2.5 mL) and cooled to 0 °C. Then triphenylphosphine (170 mg, 0.650 mmol) and *tert*-butyl (*S*)-2-hydroxybutyrate (104 mg, 0.650 mmol) were then added, followed by diethylazodicarboxylate (102 μL, 0.650 mmol). The reaction was stirred overnight and then directly purified by silica gel chromatography to give 275 mg of the title compound. ^{1}H NMR (500 MHz, $CDCl_3$): δ 7.84 (d, Ph, J = 8.9 Hz, 2H), 7.49 (t, Ph, 1H), 7.45 (d, Ph, J = 8.7 Hz, 1H), 7.05 (br, Ph, 1H), 6.97 (m, Ph, 4H), 6.89 (br, Ph, 1H), 6.87 (br t, Ph, 1H), 4.50 (t, O<u>CH</u>(CH_2CH_3)CO_2tBu, 1H), 3.90 (s, OCH3, 3H), 2.37 (s, 2-CH_3, 3H), 2.01 (m, OCH(<u>CH_2</u>CH_3)CO_2tBu, 2H), 1.47 (br s, OCH(CH_2CH_3)CO_2t<u>Bu</u>, 9H), 1.10 (t, OCH(CH_2<u>CH_3</u>)CO_2tBu, 3H). LC/MS: *m*/*e* 584.12 (M + 1).

(2*R*)-2-(3-{3-[(4-Methoxyphenyl)carbonyl]-2-methyl-6-(trifluoromethoxy)-1*H*-indol-1-yl}phenoxy)butanoic Acid (6). First, 274 mg (0.470 mol) of (**12**) was dissolved in 4.7 mL of dichloromethane. Then trifluoroacetic acid (2.4 mL, 31.1 mol) was added and the reaction was stirred until TLC monitoring showed that the reaction was complete. The volatiles were removed by rotary evaporation. The residue was dissolved twice in dichloromethane/hexanes and evaporated. The residue was pumped on high vacuum for 12 h. It was purified on a silica gel column (70/30/0.33 hexanes/ethyl acetate/acetic acid) to give clean title compound (236 mg, 95% yield) after isolation. ^{1}H NMR (500 MHz, $CDCl_3$): δ 7.84 (d, Ph, J = 8.7 Hz, 2H), 7.50 (t, Ph, 1H), 7.42 (br s, Ph, 1H), 7.08 (br s, Ph, 1H), 6.970 (m, Ph, 4H), 6.92 (br m, Ph, 2H), 4.67 (br m, O<u>CH</u>(CH_2CH_3)CO_2H, 1H), 3.90 (s, OCH_3, 3H), 2.38 (s, 2-CH_3, 3H), 2.07 (m, OCH(<u>CH_2</u>CH_3)CO_2H, 2H), 1.13 (t, OCH(CH_2-<u>CH_3</u>)CO_2H, 3H). LC/MS: *m*/*e* 528 (M + 1). HRMS: *m*/*e* 528.1614 (M + 1) calcd (M + 1) 528.1644. HPLC purity 99.7% (t_R = 2.316 min). Chiral purity 99.6% t_R13.19 min, 0.1% t_R 19.24 min (racemate 50/50 at t_R 13.22 and 19.25 min, respectively).

Preparation of Recombinant PPARs and Binding Assay. Recombinant PPARs were prepared and the receptor binding assays were performed as previously described.[15] Briefly, the full length human cDNAs for each was subcloned into pGEX-KT expression

vectors (Pharmacia, Piscataway, NJ), followed by production of purified recombinant proteins in *Escherichia coli*. Using the purified GST-hPPAR receptors, scintillation proximity assay-based receptor competitive binding assays were performed in Packard OptiPlate-96 well polystyrene microplates (Packard BioScience, Meriden, CT) using [$^3H_2$]nTZD3 for PPARγ and PPARα and [$^3H_2$]nTZD4 for PPARδ. K_is were calculated by the equation of Cheng and Prusoff.[28] Four-parameter logistic equation used is shown below:

$$Y = \text{Bottom} + (\text{Top} - \text{Bottom})/1 + (\text{LogEC}_{50} - X)\text{HillSlope} \quad (1)$$

Bottom is the Y value at the bottom plateau, while Top is the Y value at the top plateau. Log EC_{50} is the X value when the response is halfway between bottom and top. HillSlope describes the steepness of the curve (GraphPad Prism version 4.00 for Windows, GraphPad Software, Inc., San Diego, CA).

Cell-Based Transcriptional Activity Assays. COS-1 cells were cultured and transactivation assays were performed as previously described.[26] Briefly, cells were transfected with a pcDNA3-hPPAR/GAL4 expression vector, pUAS(5X)-tk-luc reporter vector, and pCMV-lacz as an internal control for transactivation efficiency using Lipofectamine (Invitrogen, Carlsburg, CA). After a 48 h exposure to compounds, cell lysates were produced, and luciferase and β-galactosidase activity in cell extracts were determined. Inflection points (EC_{50}) of normalized luciferase activity were calculated by the four-parameter logistic equation.

Gene Signature Profiling in 3T3-L1 Cells. 3T3-L1 cells were grown to confluence in medium A (Dulbecco's modified Eagle's medium with 10% fetal calf serum, 100 units/mL penicillin, and 100 μg/mL streptomycin) at 37 °C in 5% CO_2 and induced to differentiate as previously described.[29] Briefly, differentiation was induced by incubating the cells with medium A supplemented with methylisobutylxanthine (IBMX), dexamethasone, and insulin for 2 days (days 1 to 2), followed by another 2-day incubation with medium A supplemented with insulin (days 3 to 4). The cells were further incubated in medium A for an additional 4 days to complete the adipocyte conversion (days 5 to 8). At day 8 following the initiation of differentiation, cells were incubated in medium A ± compounds for 24 h at saturating concentrations: vehicle, rosiglitazone (600nM), COOH (3870 nM), or SPPARγM6 (1075 nM). The doses were chosen to be 1.5 log the inflection point in the fatty acid binding protein adipogenesis assay performed in 3T3-L1 cells. Following treatment, total RNA was prepared from the adipocytes using Trizol reagent (Invitrogen, Carlsbad, CA) and RNeasy kits (Qiagen, Valencia, CA) according to the manufacturers' instructions and RNA concentration was estimated from absorbance at 260 nm. Microarray processing was performed as previously described.[30,31] Briefly, labeled cRNA was hybridized for 48 h onto Agilent 60mer 2-color spotted microarrays. Individual treatment samples (including individual vehicle treatment samples) were hybridized against a vehicle treatment pool. LogRatio and P values were generated by averaging replicates (3 replicates per treatment) and the Rosetta Resolver v7.2 system (Rosetta Inpharmatics LLC, a wholly owned subsidiary of Merck and Co., Inc., Seattle, WA). LogRatio values represent the difference in regulation of the compound treated samples versus the vehicle treated sample where a positive value signifies up-regulation following compound treatment and vice versa. A PPARγ activity score indicative of overall adipoctye gene expression was generated using a subset of 4619 reporter genes and the χ-square fitting approach, as previously described.[23] This subset of reporter genes is composed of the intersection of the two PPARγ full agonists, rosiglitazone and COOH signature reporter genes with $P < 0.01$.

Glucose Measurements. *db*/*db* mice were used as described previously.[28]

Adiponectin Measurements. Serum/Plasma Sample Handling. Serum 5−15 μL per sample of plasma were received. Vehicle was diluted 1:1000 μL into 5 mL of 1× assay buffer (10 mM phosphate buffer, pH 7.6 containing 0.08% sodium azide, 0.1% RIA grade BSA), and all full and partial agonists were diluted either 1:1000 or 1:5000, 1, or 5 μL into 5 mL of 1× assay buffer. Each sample was assayed in duplicate.

Assay Protocol. The assay utilized a Mouse Adiponectin RIA kit (cat. no. MADP-60HK) purchased from LINCO Research, Inc. St. Charles, MO. The assay was performed over 2 days and utilizes ^{125}I-labeled murine adiponectin and a multispecies adiponectin rabbit antiserum to determine the level of adiponectin in serum, plasma, or tissue culture media by the double antibody/PEG technique. The adiponectin standards were prepared using recombinant mouse adiponectin and were used to determine the μg/mL circulating levels of adiponectin in plasma samples.

Adiponectin Concentration Determination. The concentrations of adiponectin in the plasma samples were determined from the standard curve, which was linear from 1 to 100 ng/mL. Standards are fit to a one site competition equation using GraphPad Prism Software purchased from GraphPad Software, Inc., San Diego, CA.

Statistical Analysis. The unknown concentrations of adiponectin determined by GraphPad Prism Software were exported to the CMG (Comparing Multiple Groups) Guidance System statistical package, provided by the Merck Biometrics Research Department. This provided all statistical data, including point and box plot graphs, along with pairwise comparison results.

Obese Zucker *fa*/*fa* Rat Studies. Nine−ten week old male Zucker *fa*/*fa* rats (Charles River Laboratories, Wilmington, MA) were housed two animals per cage and were provided food (Harlan Teklad Diet no. 7012, Madison, WI) and water ad libitum. Animals were housed in a temperature-, humidity-, and light-controlled room (21−23 °C, 47−65%, 12−12 h light−dark cycle, $n = 8$/group). Following 7 days of acclimation, rats were treated once daily for 7 days by oral gavage with vehicle (0.25% methylcellulose, 10 mL/kg), rosiglitazone (0.1, 1, 10, and 100 mg/kg), or SPPARγM 6 (3, 30, 100, and 150 mg/kg).

Evaluation of Insulin Sensitization. Tail nick blood samples were collected one day before the start of dosing and one day after seventh dose and plasma glucose (Sigma glucose Trinder assay kit, St. Louis, MO), insulin (rat insulin RIA from American Laboratory Products Company, Windham, NH), free fatty acids (FFA) and triglyceride (both from Roche Diagnostics, Basel, Switzerland) concentrations were determined.

Bioelectrical Impedance Analysis for Determination of Extracellular Fluid Volume. Twenty-four hours following the final dose, rats were anesthetized with ketamine (85 mg/kg, im) and xylazine (10 mg/kg, im). Animals were positioned on a nonconductive surface in dorsolateral recumbency and *extracellular fluid* volume was determined by bioelectrical impedance analysis, following procedures described by the manufacturer (Hydra ECF/ICF impedance analyzer model 4, Xitron, San Diego, CA) and by B. H. Cornish et al.[32] and Rutter et al.[33] A tetrapolar impedance monitor was used to measure impedance, and hence the total body water, over a frequency range of 5 kHz to 1 MHz. Source electrodes (1 cm × 26G stainless steel needles) were inserted 5 mm subcutaneously. Detector electrodes were inserted along the midline at the anterior point of the sternum and the anterior point of the penis. The distance between electrodes was measured and included for data modeling.

Plasma Volume Measurement. After determination of *extracellular fluid* volume, plasma volume was measured in anesthetized animals using a dye dilution technique following methods described by Belcher and Harriss[34] with minor modifications. Evans blue dye solution (25 mg/mL in physiological saline) was filtered through a 0.22 μm filter prior to injection into a femoral vein. Twenty minutes after injection, a heparinized blood sample (2 mL) was withdrawn from the descending aorta. Plasma was separated by centrifugation of the blood at 1100*g* for 15 min.; samples were kept at −80 °C until assayed. Absorbance of the thawed plasma was read at 620 nm, and plasma Evans blue dye concentrations were calculated according to a standard curve generated by a serial dilution of the 25 mg/mL Evans blue dye−saline solution. Plasma volume was calculated by using the dilution factors of Evans blue as shown below.

plasma volume = [dye] × volume of dye injected/ [dye]in plasma (2)

Heart Weight Measurements. Animals were then euthanized by pneumothorax and exsanguination, and the heart was excised, blotted, and weighed.

Plasma Drug Level Measurements. All plasma samples collected from the descending aorta were precipitated with acetonitrile and subsequently subject to LC/MS/MS for rosiglitazone and SPPARγM **6** measurements.

Animal Care and Handling. All animal experiments and euthanasia protocols were conducted in strict accordance with the National Research Council's *Guide for the Care and Use of Laboratory Animals*. Animal experiment protocols were reviewed and approved by the Institutional Animal Care and Use Committee of Merck Research Laboratories. The laboratory animal facilities of Merck Research Laboratories are certified by the Association for Assessment and Accreditation of Laboratory Animal Care International.

Statistical Analysis. Data were expressed in one of the three ways as noted in legends or footnotes: mean ± SEM, or mean ± SD. Dunnett's *t* test was performed to determine if there were significant differences between the vehicle group and each incremental dosage group of a compound for the following parameters: plasma glucose, triglyceride, free fatty acids and insulin concentration, plasma volume, extracellular fluid volume, and hematocrit. A P value <0.05 was considered statistically significant.

Acknowledgment. We thank Renee M. Chabin, Bahanu Habulihaz, the Rosetta Gene Expression Laboratory, and Neelam Sharma for additional technical support.

References

(1) Plosker, G. L.; Faulds, D. Troglitazone: A Review of its Use in the Management of Type 2 Diabetes Mellitus. *Drugs* **1999**, *57*, 409–438.
(2) Balfour, J. A.; Plosker, G. L. *Rosiglitazone Drugs* **1999**, *57*, 921–930.
(3) Nesto, R. W.; Bell, D.; Bonow, R. O.; Fonseca, V.; Grundy, S. M.; Horton, E. S.; Winter, M. L.; Porte, D.; Semenkovich, C. F.; Smith, S.; Young, L. H.; Kahn, R. Thiazolidinedione Use, Fluid Retention, and Congestive Heart Failure: A Consensus Statement from the American Heart Association and American Diabetes Association. *Diabetes Care* **2004**, *27*, 256–263.
(4) Pickavance, L. C.; Tadayon, M.; Widdowson, P. S.; Buckingham, R. E.; Wilding, J. P. H. Therapeutic index for rosiglitazone in dietary obese rats: separation of efficacy and haemodilution. *Br. J. Pharmacol.* **1999**, *128*, 1570–1576.
(5) Richter, B.; Bandeira-Echtler, E.; Bergerhoff, K.; Clar, C.; Ebrahim, S. H. Rosiglitazone for type 2 diabetes mellitus. *Cochrane Libr.* **2007**, *3*, 1–83.
(6) Kahn, S. E.; Haffner, S. M.; Heise, M. A.; Herman, W. H.; Holman, R. R.; Jones, N. P.; Kravitz, B. G.; Lachin, J. M.; O'neill, M. C.; Zinman, B.; Viberti, G. Glycemic Durability of Rosiglitazone, Metformin, or Glyburide Monotherapy. *N. Engl. J. Med.* **2006**, *355*, 2427–2443.
(7) Kahn, S. E.; Zinman, B.; Lachin, J. M.; Haffner, S. M.; Herman, W. H.; Holman, R. R.; Kravitz, B. G.; Yu, D.; Heise, M. A.; Aftring, R. P.; Viberti, G. Rosiglitazone-Associated Fractures in Type 2 Diabetes: An Analysis from a Diabetes Outcome Progression Trial (ADOPT). *Diabetes Care* **2008**, *31*, 845–851.
(8) Hampton, T. Diabetes Drugs Tied to Fractures in Women. *JAMA, J. Am. Med. Assoc.* **2007**, *297*, 1645.
(9) Reginato, M. J.; Bailey, S. T.; Krakow, S. L.; Minami, C.; Ishii, S.; Tanaka, H.; Lazar, M. A. A Potent Antidiabetic Thiazolidinedione with Unique Peroxisome Proliferator-Activated Receptor γ-Activating Properties. *J. Biol. Chem.* **1998**, *273*, 32679–32684.
(10) Oberfield, J. L.; Collins, J. L.; Holmes, C. P.; Goreham, D. P.; Cooper, J. P.; Cobb, J. E.; Lenhard, J. M.; Hull-Ryde, E. A.; Mohr, C. P.; Blanchard, S. G.; Parks, D. J.; Moore, L. B.; Lehmann, J. M.; Plunket, K.; Miller, A. B.; Milburn, M. V.; Kliewer, S. A.; Willson, T. M. A peroxisome proliferator-activated receptor γ ligand inhibits adipocyte differentiation. *Proc. Nat. Acad. Sci. U.S.A.*, **1999**, *96*, 6102–6106.
(11) Elbrecht, A.; Chen, Y.; Adams, A.; Berger, J.; Griffin, P.; Klatt, T.; Zhang, B.; Menke, J.; Zhou, G.; Smith, R. G.; Moller, D. E. L-764406 Is a Partial Agonist of Human Peroxisome Proliferator-Activated Receptor γ. The Role of CYS313 in Ligand Binding. *J. Biol. Chem.* **1999**, *27*, 7913–7922.
(12) Shimaya, A.; Kurosaki, E.; Nakano, R.; Hirayama, R.; Shibasaki, M.; Shikama, H. The novel hypoglycemic agent YM440 normalizes hyperglycemia without changing body fat weight in diabetic *db*/*db* mice. *Metabolism* **2000**, *49*, 411–417.
(13) Rocchi, S.; Picard, F.; Vamecq, J.; Gelman, L.; Poitier, N.; Zeyer, D.; Dubuquoy, L.; Bac, P.; Champy, M.-F.; Plunket, K. D.; Leesnitzer, L. M.; Blanchard, S. G.; Desreumaux, P.; Moras, D.; Renaud, J.-P.; Auwerx, J. A Unique PPARγ Ligand with Potent Insulin-Sensitizing Yet Weak Adipogenic Activity. *Mol. Cell* **2001**, *8*, 737–747.
(14) Thor, M.; Beierlein, K.; Dykes, G.; Gustovsson, A.-L.; Heidrich, J.; Jendeberg, L.; Lindqvist, B.; Pegurier, C.; Roussel, P.; Slater, M.; Svensson, S.; Sydow-Bachmann, M.; Thornstrom, U.; Uppenberg, J. Synthesis and pharmacological evaluation of a new class of peroxisome proliferator-activated receptor modulators. *Bioorg. Med. Chem. Lett.* **2002**, *12*, 3565–3567.
(15) Berger, J. P.; Petro, A. E.; McNaul, K. L.; Kelly, L. J.; Zhang, B. B.; Richards, K.; Elbrecht, A.; Johnson, B. A.; Zhou, G.; Doebber, T. W.; Biswas, C.; Parikh, M.; Sharma, N.; Tanen, M. R.; Thompson, G. M.; Ventre, J.; Adams, A. D.; Mosley, R.; Surwit, R. S.; Moller, D. E. Distinct Properties and Advantages of a Novel Peroxisome Proliferator-Activated Protein-γ Selective Modulator. *Mol. Endocrinol.* **2003**, *17*, 662–676.
(16) Schupp, M.; Janke, J.; Clasen, R.; Unger, T.; Kintscher, U. Angiotensin Type 1 Receptor Blockers Induce Peroxisome Proliferator-Activated Receptor-γ Activity. *Circulation* **2004**, *109* (17), 2054–2057.
(17) Minoura, H.; Takeshita, S.; Ita, M.; Hirosumi, J.; Mabuchi, M.; Kawamura, I.; Nakajima, S.; Nakayama, O.; Kayakiri, H.; Oku, T.; Ohkubo-Suzuki, A.; Fukagawa, M.; Kojo, H.; Hanioka, K.; Yamasaki, N.; Imoto, T.; Kobayashi, Y.; Mutoh, S. Pharmacological characteristics of a novel nonthiazolidinedione insulin sensitizer, FK614. *Eur. J. Pharmacol.* **2004**, *494*, 273–281.
(18) Burgermeister, E.; Schnoebelen, A.; Flament, A.; Benz, J.; Stihle, M.; Gsell, B.; Rufer, A.; Kuhn, B.; Marki, H. P. A Novel Partial Agonist of Peroxisome Proliferator-Activated Receptor-γ (PPARγ) Recruits PPARγ-Coactivator-1α, Prevents Triglyceride Accumulation, and Potentiates Insulin Signaling in Vitro. *Mol. Endocrinol.* **2006**, *20*, 809–830.
(19) Acton, J. J.; Black, R. M.; Jones, A. B.; Moller, D. E.; Colwell, L.; Doebber, T. W.; MacNaul, K. L.; Berger, J.; Wood, H. B. Benzoyl 2-methyl indoles as selective PPARγ modulators. *Bioorg. Med. Chem. Lett.* **2005**, *15*, 357–362.
(20) Liu, K.; Black, R. M.; Acton, J. A., III; Mosley, R.; Debenham, S.; Abola, R.; Yang, M.; Tschirret-Guth, R.; Colwell, L.; Liu, C.; Wu, M.; Wang, C. F.; MacNaul, K. L.; McCann, M. E.; Moller, D. E.; Berger, J. P.; Meinke, P. T.; Jones, A. B.; Wood, H. B. Selective PPARγ modulators with improved pharmacological profiles. *Bioorg. Med. Chem. Lett.* **2005**, *15*, 2437–2440.
(21) Einstein, M.; Akiyama, T. E.; Castriota, G. A.; Wang, C. F.; McKeever, B.; Mosley, R. T.; Becker, J. W.; Moller, D. E.; Meinke, P. T.; Wood, H. B.; Berger, J. P. The Differential Interactions of Peroxisome Proliferator-Activated Receptor γ Ligands with Tyr473 Is a Physical Basis for Their Unique Biological Activities. *Mol. Pharmacol.* **2008**, *73*, 62–74.
(22) Kumar, S.; Kelem, K.; Tschirret-Guth, R.; Mitra, K.; Baillie, T. Minimizing metabolic activation during pharmaceutical lead optimization: Progress, knowledge gaps and future directions. *Curr. Opin. Drug Discovery Dev.* **2008**, *11* (1), 43–52.
(23) Chang, C. H.; McNamara, L. A.; Wu, M. S.; Muise, E. S.; Tan, Y.; Wood, H. B.; Meinke, P. T.; Thompson, J. R.; Doebber, T. W.; Berger, J. P.; McCann, M. E. A novel selective peroxisome proliferator-activator receptor-gamma modulator-SPPARγM5 improves insulin sensitivity with diminished adverse cardiovascular effects. *Eur. J. Pharmacol.* **2008**, *584*, 192–201.
(24) Gassman, P. G.; van Bergen, T. J. Simple method for the conversion of anilines into 2-substituted indoles. *J. Am. Chem. Soc.* **1973**, *95*, 590–591.
(25) Acton, J. J., Debenham, S. D., Liu, K., Meinke, P. T., Wood, H. B. Indoles having anti-diabetic activity. Patent WO2004/020408 A1, 2004.
(26) Berger, J. B.; Leibowitz, M. D.; Doebber, T. D.; Elbrecht, A.; Zhang, B.; Zhou, G.; Biswas, C.; Cullinan, C. A.; Hayes, N. S.; Li, Y.; Tanen, M.; Ventre, J.; Wu, M. S.; Berger, G. D.; Mosley, R.; Marquis, R.; Santini, C.; Sahoo, S. P.; Tolman, R. L.; Smith, R. G.; Moller, D. E. Novel Peroxisome Proliferator-Activated Receptor (PPAR)γ and PPARδ Ligands Produce Distinct Biological Effects. *J. Biol. Chem.* **1999**, *274*, 6718–6725.
(27) Tugwoog, J. D.; Montegue, C. T. Biology and toxicology of PPAR-gamma ligands. *Hum. Exp. Toxicol.* **2002**, *21*, 429–437.
(28) Berger, J.; Bailey, P.; Biswas, C.; Cillinana, C. A.; Doebber, T. W.; Hayes, N. S.; Saperstein, R.; Smith, R. G.; Liebowitz, M. D. Thiazolidinediones produce a conformational change in peroxisomal proliferator-activated receptor-gamma: binding and activation correlate with antidiabetic actions in *db*/*db* mice. *Endocrinology* **1996**, *137*, 4189–4195.

(29) Cheng, Y.; Prusoff, W. H. Relationship between the inhibition constant (K_i) and the concentration of the inhibitor which causes 50% inhibition (IC_{50}) of an enzyme reaction. *Biochem. Pharmacol.* **1973**, *22*, 3099–3108.

(30) Zhang, B.; Berger, J. B.; Zhou, G.; Elbrecht, A.; Biswas, S.; White-Carrington, S.; Szalkowski, D.; Moller, D. E. Insulin- and mitogen-activated protein kinase mediated phosphorylation and activation of peroxisome proliferator-activated receptor-γ. *J. Biol. Chem.* **1996**, *271*, 31771–31774.

(31) Hughs, T. R.; Mao, M.; Jones, A. R.; Burchard, J.; Marton, M. J.; Shannon, K. W.; Lefkowitz, S. M.; Ziman, M.; Schelter, J. M.; Meyer, M. R.; Kobayashi, S.; Davis, C.; Dai, H.; He, Y. D.; Stephaniants, S. B.; Cavet, G.; Walker, W. L.; West, A.; Coffey, E.; Shoemaker, D. D.; Stoughton, R.; Blanchard, A. P.; Friend, S. H.; Linsley, P. S. Expression profiling usng microarrays fabricated by ink-jet oligonucleotide synthesizer. *Nat. Biotechnol.* **2001**, *19*, 342–347.

(32) Cornish, B. H.; Ward, L. C.; Tonas, B. J.; Jebb, S. A.; Elia, M. Evaluation of multiple frequency bioelectrical impedance and Cole−Cole analysis for the assessment of body water volumes in healthy humans. *Eur. J. Clin. Nutr.* **1996**, *50*, 159–164.

(33) Rutter, K.; Hennoste, L.; Ward, L. C.; Cornish, B. H.; Thomas, B. J. Bioelectrical impedance analysis for the estimation of body composition in rats. *Lab. Anim.* **1998**, *32*, 65–71.

(34) Belcher, E. H.; Harriss, E. B. Studies of plasma volume, red cell volume and total blood volume in young growing rats. *J. Physiol.* **1957**, *139*, 64–78.

JM900097M